Ab initio Calculations of the Electric Field Gradients in Solids in Relation to the Charge Distribution *

Karlheinz Schwarz and Peter Blaha

Institut für Technische Elektrochemie, Technische Universität Wien, Vienna, Austria

Z. Naturforsch. **47a**, 197–202 (1992); received August 3, 1991

A first principles method for the computation of electric field gradients (EFGs) is illustrated for various solids. This scheme is based on self-consistent energy band-structure calculations by the *full potential linearized augmented plan wave* (FLAPW) method which provides the electronic charge density including all polarization effects. By numerically solving Poisson's equation we obtain the Coulomb potential in a form which allows to compute the EFG directly. Our method is demonstrated for insulators (Cu_2O), metals (hcp-Zn), superconductors ($YBa_2Cu_3O_7$) and molecular crystals (Cl_2, Br_2, I_2).

Key words: Band-structure calculation, Electric field gradient, Nuclear quadrupole interaction, Molecular crystals, High-T_c superconductors.

Introduction

The electric field gradient (EFG) is a ground state property of a system and depends sensitively on the asymmetry of the electronic charge distribution. The EFG can be measured by various experimental techniques, which allow to extract the nuclear quadrupole interaction (NQI), such as nuclear-magnetic resonance (NMR), nuclear quadrupole resonance (NQR), Mössbauer, or perturbed angular correlation (PAC) spectroscopy. All nuclei with a nuclear-spin quantum number $I \geq 1$ have a non-spherical nuclear charge distribution and thus an electric quadrupole moment Q. The NQI between this Q and the electric field gradient (EFG) determines the nuclear quadrupole coupling constant (NQCC) e^2Qq/h, where e is the electric charge,, h is Planck's constant and q represents the EFG. The EFG is defined as the second derivative of the electrostatic potential at the nuclear position written as traceless tensor [1]. Experimentally one can determine the NQCC so that only the product Q times q is available. Often the atomic value Q(i) of nucleus i is not well known experimentally, so that one reslies on theory. Pyykkö [2] has used new fully numerical methods for atoms and small molecules to compute reliable EFGs. With these calculated q's and the experimental NQCCs he determined the nuclear quadrupole moments Q, so far of the light elements up to $Z = 20$. We choose another example for molecular EFGs, and mention Palmer [3], who compared experimental NQCC with his EFG calculations performed by the Hartree-Fock (plus configuration interaction) method using extended basis sets. These computations are for atoms and molecules, but in the present paper we focus on solids.

* Presented at the XIth International Symposium on Nuclear Quadrupole Resonance Spectroscopy, London, U.K., July 15–19, 1991.

Reprint requests to Prof. Dr. Karlheinz Schwarz, Institut für Technische Elektrochemie, Technische Universität Wien, Getreidemarkt 9/158, A-1060 Wien, Austria.

The Electric Field Gradient Formalism

The general expression for the principal component of the *electric field gradient* (EFG) tensor arising from a (nuclear plus electronic) charge density $\varrho(r)$ is defined as

$$V_{zz} = \int \varrho(r) \frac{2P_2(\cos\vartheta)}{r^3} \, \mathrm{d}r \,, \tag{1}$$

where P_2 is the second-order Legendre polynomial. Once the charge density of a system is known to high precision, the EFG can be obtained numerically form (1) without further approximations (such as Sternheimer antishielding factors). For the earlier work the reader is referred to the review article by Kaufman and Vianden [4] and that by Das and Schmidt [5] covering the theoretical aspects.

In solids the electronic structure is commonly determined in the framework of *density functional theory*

0932-0784 / 92 / 0100-0197 $ 01.30/0. – Please order a reprint rather than making your own copy.

based on the Hohenberg-Kohn-Sham formalism. The complicated many-electron system of a solid including the important exchange and correlation effects is replaced by an iso-electronic reference system of non-interacting electrons, which has the same (spin) densities as the real system. This is made possible by the *local (spin) density approximation* (LDA) which leads to a Schrödinger-like one-electron equation with a local potential. Once these (so-called) Kohn-Sham equations are solved self-consistently the charge density contains all ionic, covalent, and polarization effects in the solid. No assumptions are made about ionicities or specific charge distributions.

In 1985 Blaha, Schwarz and Herzig [6] developed a first principles method to compute EFGs from an all electron band-structure calculation following the lines indicated above. They have used the full potential linearized augmented plane wave (LAPW) method and have calculated the EFG directly from the self-consistent charge density by solving Poisson's equation. In the meantime our computer program is published as WIEN-code [7], where additional references to the LAPW method and the LDA can be found. The formalism has been described by Herzig [8] and in connection with various applications [9–12]. A short summary of the essential equations is given below:

In the LAPW scheme the unit cell is divided into non-overlapping atomic spheres (with radii R_t) and in an interstitial region; inside the spheres the charge density (and analogously the potential) is written as radial function $\varrho_{\mathrm{LM}}(r)$ times symmetrized spherical harmonics $Y_{\mathrm{LM}}(\hat{r})$ (crystal harmonics) and in the interstitial region as Fourier series:

$$\varrho(r) = \begin{cases} \sum\limits_{\mathrm{LM}} \varrho_{\mathrm{LM}}(r)\, Y_{\mathrm{LM}}(\hat{r}) & \text{inside sphere,} \\ \sum\limits_{K} \varrho(K)\, e^{iKr} & \text{interstitial.} \end{cases} \tag{2}$$

The charge density coefficients $\varrho_{\mathrm{LM}}(r)$ can be obtained from the wave functions by (in a shorthand notation)

$$\varrho_{\mathrm{LM}}(r) = \sum_{E_{nk}<E_{\mathrm{F}}} \sum_{lm} \sum_{l'm'} R_{lm}(r)\, R_{l'm'}(r)\, G^{\mathrm{M}mm'}_{\mathrm{L}ll'}, \tag{3}$$

where $G^{\mathrm{M}mm'}_{\mathrm{L}ll'}$ are Gaunt numbers and $R_{lm}(r) = A_{lm}\, u_l(r) + B_{lm}\, \dot{u}_l(r)$ denote the LAPW radial wave functions (of state E_{nk}) in the standard notation [7].

For a given charge density the Coulomb potential is obtained numerically by solving Poisson's equation in form of a boundary value problem using a method proposed by Weinert [13]. This yields the potential coefficients $v_{\mathrm{LM}}(r)$ in analogy to (2). For the EFG calculation only the $L=2$ terms near the nucleus are needed; in the limit $r \to 0$ the asymptotic form of the potential $r^L\, V_{\mathrm{LM}}\, Y_{\mathrm{LM}}$ can be used, and this procedure yields (see [11])

$$\begin{aligned} V_{2\mathrm{M}} = &-C_{2\mathrm{M}} \int_0^R (\varrho_{2\mathrm{M}}(r)/r^3)\, r^2\, \mathrm{d}r \\ &+ C_{2\mathrm{M}} \int_0^R \varrho_{2\mathrm{M}}(r)\,(r/R)^5/r\, \mathrm{d}r \\ &+ 5\, C_{2\mathrm{M}}/R^2 \sum_K V(K)\, j_2(KR)\, Y_{2\mathrm{M}}(K) \end{aligned} \tag{4}$$

with $C_{20} = 2(4\pi/5)^{1/2}$, $C_{22} = (3/4)^{1/2} C_{20}$, and the spherical Bessel function j_2. The first term (called *valence* EFG) corresponds to the integral of (1) taken over the atomic sphere; after integration over ϑ and φ a radial integration must be carried out. The second and third term (called *lattice* EFG) arise from the boundary value problem and from charge contributions outside the considered sphere. Note that our definition of the lattice EFG differs from that based on a point charge model [4]. With these definitions the diagonal terms of the traceless EFG tensor with respect to the crystallographic axis a, b, and c are

$$\begin{aligned} V_{aa} &= -\tfrac{1}{2} V_{20} + V_{22}\,, \\ V_{bb} &= -\tfrac{1}{2} V_{20} - V_{22}\,, \\ V_{cc} &= V_{20}\,. \end{aligned} \tag{5}$$

In many simple cases the off-diagonal elements of the EFG tensor vanish due to symmetry, but if non-diagonal terms exist diagonalization of the EFG tensor is required. By ordering the components according to their magnitudes we define

$$|V_{zz}| \geq |V_{yy}| \geq |V_{xx}|\,. \tag{6}$$

The EFG tensor is characterized by the largest component V_{zz} (in short EFG) and the anisotropy parameter η defined as

$$\eta = (V_{xx} - V_{yy})/V_{zz}\,, \tag{7}$$

where η varies between 0 (axial symmetry) and 1 ($V_{xx}=0$).

Results and Discussion

In the present paper we restrict ourselves to results obtained by this new approach which has been applied to various solids, from insulators such as Li_3N

[6] or Cu_2O [9], to (hcp) metals [10] and to high temperature superconductors as $YBa_2Cu_3O_{6+x}$ [11] and resently to $YBa_2Cu_4O_8$ [12]. The series of systems has been extended to molecular crystals such as Cl_2, Br_2, and I_2 for which we studied solid state effects [14]. From each class an example is chosen so that various features can be illustrated. For further details (computation, references, interpretation) the reader is refered to the original papers.

Ionic Solids: Cuprite, Cu_2O

Instead of choosing Li_3N to which the new method was first applied we select cuprite as example for an ionic crystal. Cu_2O crystallizes in a simple cubic structure and can be crudely described to consist of Cu^+ and O^{2-} ions. The electronic structure has been obtained by an LAPW band structure calculation [15] which showed that Cu has not the simple $3d^{10}$ configuration, but less than 10d electrons. This causes an asymmetry in the charge distribution around the Cu site which can best be illustrated by looking at the difference density obtained between the crystalline density and a superposition of ionic densities (see Fig. 6b of [15]).

Based on this LAPW calculation the EFG was computed using the new formalism [9]. This system is chosen as an example to illustrate the various terms contributing to the EFG. According to (5) the EFG is given by the V_{LM} defined in (4), whose first term is called *valence* (coming from inside the atomic sphere) and the remainder is termed *lattice* EFG. Table 1 shows that the lattice contribution is rather small in contrast to the term from inside the sphere. Then we raise the question, which states contribute to the latter. The valence electrons (Cu-3d and 4p) clearly dominate over the semi-core states (Cu-3p), so that the polarization of the true core states (Cu 1s, 2s, 2p) can be neglected. Another decomposition is usefull: according to (3) and the selection rules for the Gaunt numbers the required density $\varrho_{20}(r)$ can come only from a combination of radial functions $R_{lm}(r)$ with p-p, d-d or s-d character (omitting high l-terms which are negligible). Thus we can write

$$\varrho_{20}(r) = \varrho_{20}^{pp}(r) + \varrho_{20}^{dd}(r) + \varrho_{20}^{sd}(r)\,, \tag{8}$$

where the latter turns out to be extremely small and is therefore omitted in the analysis shown below. With these definitions we can further decompose the valence contribution to the EFG into p-p and d-d terms

Table 1. EFG contributions for Cu in Cu_2O [9], Cu(2) in $YBa_2Cu_3O_7$ [11] and hcp-Zn [10] (top panel) and relation between EFG (10^{21} V/m^2), asymmetry count Δn_l and moment M_l (proportional to $\langle 1/r^3 \rangle$) from p and d states; for definition see text. The references to the many experimental data can be found in the original papers [9–11].

		Cu_2O	$YBa_2Cu_3O_7$	hcp-Zn
EFG	lattice	0.1	−0.1	−0.0
	semi-core	0.9	−0.2	−0.6
	valence: p-p	−17.8	9.6	5.3
	d-d	8.5	−14.9	−1.0
		−9.3	−5.3	4.3
	theory: total	−8.3	−5.6	3.6
	experiment	±10.2	±12.3	±3.7
V_{zz}(p)		−17.8	9.6	5.3
Δn_p		−0.055	0.038	0.041
M_p		330	250	129
V_{zz}(d)		8.5	−14.9	−1.0
Δn_d		0.165	−0.288	−0.010
M_d		48	47	100

(Table 1). In the case of Cu_2O we note that the p-p term is large and has the opposite sign to the d-d contribution, but both are important for the EFG.

High Temperature Superconductors: $YBa_2Cu_3O_7$

The new class of perovskite superconductors, for which one speculates that correlation effects could play an important role, were studied intensively in order to establish how the charge is distributed. In this context EFG measurements and calculations are extremely usefull. Since details have been published before [11, 16] only a few results will be presented here. The EFGs calculated for $YBa_2Cu_3O_7$, $YBa_2Cu_3O_6$ and $YBa_2Cu_4O_8$ [12] agree well between theory and experiment in magnitude, orientation, and asymmetry parameter for all sites (Y can not be measured) with the exception of the Cu(2) position corresponding to the copper in the Cu–O layer, which will be discussed below. The EFG at the oxygen sites is easy to interprete: Table 2 gives the partial charges inside the four types of oxygen spheres indicating an asymmetry in the charge distribution which is clearly visible in the corresponding difference density $\Delta\varrho$ (see Fig. 3 of [11]). Two of the p-charges are around 1.2 electrons, while the third is significantly smaller. This asymmetry is directly related to the corresponding EFG whose principal axes point in the crystallographic directions where the p-population is smallest.

Table 2. Symmetry decomposition of the valence charges (in electrons) in the 4 oxygen spheres of $YBa_2Cu_3O_7$ in comparison to the EFG (10^{21} V/m^2), where the cartesian coordinates are assumed to be parallel to the crystallographic axes: $x \parallel a$, $y \parallel b$, $z \parallel c$.

	p_x	p_y	p_z	V_{aa}	V_{bb}	V_{cc}
O(1)	1.18	**0.91**	1.25	−6.1	**18.3**	−12.2
O(2)	**1.01**	1.21	1.18	**11.8**	−7.0	−4.8
O(3)	1.21	**1.00**	1.18	−7.0	**11.9**	−4.9
O(4)	1.18	1.19	**0.99**	−4.7	−7.0	**11.7**

Therefore the EFG can be directly related to the symmetry decomposed partial charges. In the special case of the Cu(2) position, where V_{22} is very small so that V_{20} dominates, one can split the EFG into contributions from two groups of p and three groups of d functions according to the point group symmetry. In this context it is useful to define an asymmetry count [10, 11, 16] in terms of partial charges (labeled by their symmetry)

$$\Delta n_p = 1/2(p_x + p_y) - p_z ,$$
$$\Delta n_d = (d_{xy} + d_{x^2-y^2}) - 1/2(d_{xz} + d_{yz}) - d_{z^2} . \quad (9)$$

The partial charges grouped with prefactors and signs according to (9) contribute to the asymmetry count Δn_l. These values Δn_l, the corresponding *valence* EFG (V_{zz} contribution), and the ratio $M_l = \mathrm{EFG}/\Delta n_l$ are listed in Table 1 for the p and d terms. These factors are proportional to the corresponding $\langle 1/r^3 \rangle$ expectation value as previously demonstrated [9] for Cu_2O, for which these quantities are given in Table 1 as well. The ratio for the d-d contribution M_d is about constant in Cu_2O and $YBa_2Cu_3O_7$, indicating that $\langle 1/r^3 \rangle$ expectation values do not differ significantly in these two compounds. In hcp-Zn (discussed below) the 3d wave-function is much more localized and consequently M_d for Zn is twice as large as that of copper. The M_p are larger than the M_d factors, but the values vary somewhat between Cu_2O and $YBa_2Cu_3O_7$. This comes about since the Cu-4p function is not only an on-site function, but must represent the tails of the O-2p functions which in an LCAO description would reach into the Cu sphere. An on-site 4p function as in Zn has a smaller M_p value. The EFG can be obtained directly from the partial charges, provided they are properly grouped and weighted according to (9) and multiplied by M_p or M_d.

Such an analysis allowed us to estimate that a transfer of only 0.07 electrons from $d_{x^2-y^2}$ to d_{z^2} symmetry at Cu(2) in $YBa_2Cu_3O_7$ would be sufficient to bring the theoretical EFG in agreement with the experimental EFG value. This illustrates nicely the sensitivity of the EFG with respect to the charge distribution. From that work we must conclude that the present form of the LDA is not perfect, but still provides a charge distribution that is close to reality even for the highly correlated superconductors. Furthermore, this high sensitivity allows us to quantify the charge distribution on copper within narrow limits, an important information for setting up models for superconductivity which occurs in the plane of Cu(2).

Metals: hcp Zn

Metals have been studied by various theories, for example by Pattnaik et al. [17]. The EFG for all hexagonal-closed-packed (hcp) metals from Be to Cd has been obtained with the formalism described above [10]. We have selected just one example, namely hcp Zn, to show that metals can be treated the same way as ionic solids and that often the p-p contributions are more important than the d-d term (Table 1) with the sign sometimes the same and sometimes opposite. The valence contribution again dominates and the semicore polarization adds only little to the EFG. The various contributions to the EFG and their relation of the anisotropy of the charge density has been extensively discussed in [9]. It should be pointed out that the EFG of the hcp metals is rather sensitive to the c/a ratio as was illustrated for Be [18] or Ti, Zn and In [19].

Molecular Crystals: Cl_2, Br_2, and I_2

The solid halogens are used as model compound to study solid state effects in a molecular crystal. They crystallize in an orthorhombic structure (Fig. 1) and closely resemble the isolated molecules. The empty antibonding σ^* orbitals give rise to the large EFG, which our calculation finds almost exactly in the molecular axes, although that was not required by symmetry. The asymmetry parameter of the EFG, however, comes from the intermolecular interaction, which a solid state calculation should be able to describe. Therefore we applied our method to compute the EFG and η for Cl_2, Br_2 and I_2 and summarize the results in Table 3, which shows that – according to theory – η steadily increases in this series. This result

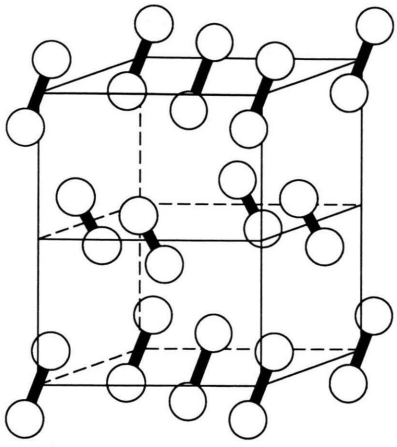

Fig. 1. Crystal structure of solid Cl_2 in the base-centered orthorhombic unit cell, space group Cmca (D_{2h}^{18}).

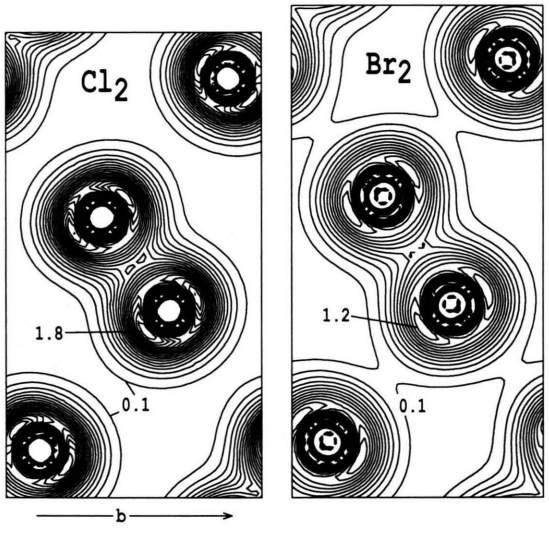

Fig. 2. Valence electron density of solid Cl_2 and Br_2 in the (100) plane, through the to *b*- and *c*-axis; the maxima and minima are contour lines in units of 0.1 e/Å^3.

Table 3. Electric field gradient of solid Cl_2, Br_2, and I_2. Most experimental data are taken from [20] except for Cl_2 as specified.

	Cl_2	Br_2	I_2
Isotope	^{35}Cl	^{79}Br	^{127}I
$Q/mb = 10^{-31}\,m^2$	−82.5	293	−789
EFG theory	+53.7	+96.6	+118.8
(10^{21} V/m^2) exp.	±54.6	±108.0	±113.0
η theory	0.07	0.19	0.32
exp.	0.06 [21]	0.20	0.18
	0.4 [22]		
	0.2 [23]		

is consistent with the ratio of the inter- to the intramolecular distances, which decrease from 1.68 over 1.46 to 1.29, so that the shorter inter-molecular distance causes η to increase. For Br_2 the agreement in η is excellent, but theory finds a larger value for I_2, while for Cl_2 the experimental η value scatters a lot. By comparing the valence electron density of Cl_2 with that of Br_2 (Fig. 2) we see that (judged by the density between the nearest neighbour molecules) the intermolecular interaction increases. This interaction introduces an additional asymmetry in the charge distribution which in turn is responsible for the increase in η. Further analysis is required and will be presented in a forthcoming publication [14].

Conclusion

Although these systems have extremely different chemical bonding, good overall agreement between our theory and experimental data for the principal EFG component, the orientation, and the asymmetry parameter has been found.

The LAPW calculations gave not only good results, but provided insight into the origin of the EFG. It is found that the asymmetry of the *valence* electron distribution close to the nucleus cause the EFG rather than *core* polarization. This asymmetry can be visualised by difference electron densities, or (after spatial integration) by symmetry decomposed partial charges, quantities directly related to chemical bonding. Further analysis allowed to distinguish between contributions from p- and d-electrons, where the former were found to substantially contribute to the EFG, even when they represent only a small fraction of all the valence electrons as for example in transition metals or their compounds. It should be noted that the p term (especially when the p-like charge is small) should be interpreted as an off-site contribution in context with the spatial representation of the wave function or electron density inside the atomic spheres. Tails of wave functions from neighbouring atoms entering an atomic sphere must be expanded in partial waves (s, p, d, etc. functions) which leads formally to p-functions, which are important for EFG calculations.

The *ab initio* method presented here requires high precision quantum-mechanical calculations and large computational effort, but is capable of calculating reliable EFGs in crystalline solids and provides physical insight into the origin of the EFG.

Acknowledgements

This project was supported by the Fonds zur Förderung der wissenschaftlichen Forschung, project number P 7063 P. Part of the calculations have been performed on the IBM 3090-400 VF of the computer center of the University of Vienna within the European Academic Supercomputing Initiative (EASI) sponsored by IBM.

[1] M. H. Cohen and F. Reif, Solid State Phys. **5,** 321 (1957), edited by F. Seitz and D. Turnbull (Academic, New York).
[2] P. Pyykkö, Z. Naturforsch. **47a,** 189 (1992).
[3] M. H. Palmer, Z. Naturforsch. **47a,** 203 (1992).
[4] E. N. Kaufmann and R. J. Vianden, Rev. Mod. Phys. **51,** 161 (1979).
[5] T. P. Das and P. C. Schmidt, Z. Naturforsch. **41a,** 47 (1986).
[6] P. Blaha, K. Schwarz, and P. Herzig, Phys. Rev. Lett. **54,** 1192 (1985).
[7] P. Blaha, K. Schwarz, P. Sorantin, and S. B. Trickey, Comp. Phys. Commun. **59,** 399 (1990).
[8] P. Herzig, Theoret. Chim. Acta (Berl.) **67,** 323 (1985).
[9] P. Blaha and K. Schwarz, Hyperfine Interact. **52,** 153 (1989).
[10] P. Blaha, K. Schwarz, and P. H. Dederichs, Phys. Rev. **B 37,** 2792 (1988).
[11] K. Schwarz, C. Ambrosch-Draxl, and P. Blaha, Phys. Rev. **B 42,** 2051 (1990).
[12] C. Ambrosch-Draxl, P. Blaha, and K. Schwarz, Phys. Rev. **B 44,** 5141 (1991).
[13] M. Weinert, J. Math. Phys. **22,** 2433 (1981).
[14] P. Blaha and K. Schwarz, Theochem. (submitted).
[15] P. Marksteiner, P. Blaha, and K. Schwarz, Z. Phys. **B** – Cond. Matter **64,** 119 (1986).
[16] C. Ambrosch-Draxl, P. Blaha, and K. Schwarz, J. Phys. Cond. Matter **1,** 4491 (1989).
[17] P. C. Pattnaik, M. D. Thompson, and T. P. Das, Phys. Rev. **16,** 5390 (1977).
[18] P. Blaha and K. Schwarz, J. Phys. F: Met. Phys. **17,** 899 (1987).
[19] P. Blaha, Hyperf. Interact. **60,** 773 (1990).
[20] Landolt-Börnstein, New Series III/20 (K. H. Hellwege and A. M. Hellwege, eds.), Springer-Verlag, Berlin 1988.
[21] F. J. Adrian, J. Chem. Phys. **38,** 1258 (1963).
[22] J. Weber, V. A. Gubanov, and A. A. V. Gibson, J. Magn. Reson. **20,** 427 (1975).
[23] S. Sengupta, G. Litzistorf, and E. A. C. Lucken, J. Magn. Reson. **41,** 169 (1980).